Journal of Applied Physics

Single charging events on colloidal particles in a nonpolar liquid with surfactant

Cite as: J. Appl. Phys. **123**, 015105 (2018); https://doi.org/10.1063/1.5012887
Submitted: 08 November 2017 . Accepted: 13 December 2017 . Published Online: 03 January 2018

Caspar Schreuer, Stijn Vandewiele, Toon Brans, Filip Strubbe, Kristiaan Neyts, and Filip Beunis

Single charging events on colloidal particles in a nonpolar liquid with surfactant

Caspar Schreuer, Stijn Vandewiele, Toon Brans, Filip Strubbe, Kristiaan Neyts, and Filip Beunis
Electronics and Information Systems, Ghent University, Technologiepark-Zwijnaarde 15, 9052 Gent, Belgium

(Received 8 November 2017; accepted 13 December 2017; published online 3 January 2018)

Electrical charging of colloidal particles in nonpolar liquids due to surfactant additives is investigated intensively, motivated by its importance in a variety of applications. Most methods rely on average electrophoretic mobility measurements of many particles, which provide only indirect information on the charging mechanism. In the present work, we present a method that allows us to obtain direct information on the charging mechanism, by measuring the charge fluctuations on individual particles with a precision higher than the elementary charge using optical trapping electrophoresis. We demonstrate the capabilities of the method by studying the influence of added surfactant OLOA 11000 on the charging of single colloidal PMMA particles in dodecane. The particle charge and the frequency of charging events are investigated both below and above the critical micelle concentration (CMC) and with or without applying a DC offset voltage. It is found that at least two separate charging mechanisms are present below the critical micelle concentration. One mechanism is a process where the particle is stripped from negatively charged ionic molecules. An increase in the charging frequency with increased surfactant concentration suggests a second mechanism that involves single surfactant molecules. Above the CMC, neutral inverse micelles can also be involved in the charging process. https://doi.org/10.1063/1.5012887

I. INTRODUCTION

Surfactants in low dielectric permittivity liquids are used in a wide array of applications such as electronic ink,[1] inkjet printing,[2] stabilization of detergents,[3] and the stabilization of colloids in supercritical fluid CO_2.[4] The surfactant is often instrumental for charging and/or stabilizing the suspension. Colloidal particles dispersed in a pure nonpolar liquid are typically weakly charged because of strong electrostatic forces associated with the low dielectric constant of nonpolar liquids. Dissociation of ionic species at the particle surface and other charge generating mechanisms are therefore energetically disfavored. For example, micrometer-sized particles in dodecane are found to have charges in the order of only a few to tens of elementary charges.[5] Surfactant molecules added to a nonpolar colloidal dispersion have a strong tendency to cover the surfaces of the dispersed particles and other interfaces with their nonpolar tails pointing towards the solvent. When the interfaces are completely covered, excess surfactant molecules are randomly dispersed in the solvent. At concentrations above the critical micelle concentration (CMC), the excess surfactant molecules tend to aggregate and form inverse micelles, which are small structures in which the nonpolar tails point outwards and the head groups face inwards. The presence of a surfactant leads in many cases to much higher electrical charges on the particles.[6] Essentially this can be understood by the ability of a surfactant to sterically stabilize charges and thus by preventing the immediate recombination of opposite charges. There are several commonly used commercial surfactants, such as SPAN,[7,8] AOT,[9,10] and OLOA 11000.[11–13] In general, the details of the charging mechanism depend on the type of particle, the solvent, and the type of surfactant. Several more detailed charging mechanisms to explain the origin of charge have been put forward;[14] Weitz[15] and Bartlett[6] propose a process of competitive adsorption of both positive and negative micelles which leads to an asymmetric adsorption of charged inverse micelles. In other work, Bartlett[16] argues that the adsorption of individual molecules rather than surfactant aggregates is a viable charging mechanism. Poovarodom and Berg[17] propose a system where charged surface groups dissociate from the particle surface in an acid-base reaction with the surfactant. A thorough review on the charging of PMMA particles in nonpolar solvents has been written by Eastoe.[18] Though the charging behavior of many specific systems has been identified, a comprehensive, predictive framework is still lacking. It is not always clear in advance what the charging behavior of a colloidal system will be, which in turn poses a challenge in developing industrial applications based on colloidal systems. Therefore, it is of interest to fully understand the effects of surfactants in general on the charge of colloidal particles and of OLOA 11000, in particular.

There are a number of challenges when investigating the charging mechanism of a particular colloidal dispersion due to added surfactant. Firstly, many experimental techniques rely on measuring the average electrophoretic mobility of many particles. Some insight into the charging mechanism can then, for example, be obtained by analyzing the dependency of this average mobility on surfactant concentration or other parameters such as particle size or water content. However, from such mobility measurements, it cannot be

distinguished whether the charge originates by dissociation of surface groups, by preferential adsorption of charged inverse micelles, or by other charging mechanisms. Another complication is the possible presence of undefined impurities and trace amounts of water.[2] It would be very useful to use a more direct measurement technique able to capture the dynamics of the charging mechanism in equilibrium or off-equilibrium, preferably with precision sufficient to observe single charging events.

In nonpolar liquids, the charge of a colloidal particle can be measured with elementary charge resolution. This was first demonstrated for freely diffusing particles in dodecane.[19] Later, the charge of optically trapped particles was also measured with elementary charge resolution[20] using optical trapping electrophoresis (OTE) or single particle optical manipulation[16] (SPOM). This technique uses an optical trap to keep a particle at a well-defined position in the liquid and simultaneously enables accurate measurement of the particle's position over long time intervals. In an electric field that varies sinusoidally with time, the particle experiences a sinusoidal drift speed with amplitude proportional to its charge. By monitoring the amplitude of the displacement at the frequency of the applied field, the particle charge can be estimated as a function of time. From measurements of elementary charging events on PMMA particles in dodecane, a charging and discharging mechanism in pure dodecane was proposed.[20]

In this paper, we use OTE to study the influence of the concentration of the surfactant OLOA 11000 on the charging dynamics and the charging rate of single PMMA particles in dodecane. The particle charge is measured with elementary charge resolution, for surfactant concentrations ranging from 0.001 wt. % to 0.05 wt. %, encompassing the CMC of about 0.005 wt. %.

II. MATERIALS AND METHODS

A. Samples

We study dispersions of colloidal PMMA microspheres in mixtures of nonpolar solvent and surfactant. The PMMA particles, synthesized by Andrew Schofield,[21] have a mean diameter of 996 nm and are coated with poly(hydroxystearic acid). The particles are added to the mixture of solvent and surfactant at a weight fraction of only 1/20000 to avoid secondary particles to diffuse into the optical trap during the measurement. The solvent is n-dodecane, having a dielectric permittivity $\varepsilon_r = 2$. The surfactant commercialized as OLOA 11000 (Chevron Oronite), containing about 50% surfactant polyisobutylene succinimide and 50% mineral oil, is added at concentrations between 0.001 wt. % and 0.05 wt. %, encompassing the CMC of OLOA 11000 in dodecane which is about 0.005 wt. %.[22] After the mixtures are prepared, they are kept on a roller bench for 24 h. Prior to the experiments, the mixture is homogenized using an ultrasonic bath for 10 s.

B. OTE setup

An inverted optical microscope (Nikon Eclipse Ti) is used to simultaneously visualize and probe a single colloidal particle (see Fig. 1). A 975 nm (IR) laser beam with power 60 mW is coupled to the microscope by a dichroic mirror (DM) and focused by a 100 X oil immersion objective (Nikon, Plan Fluor 100X, numerical aperture 1.3). Two Indium-Tin-Oxide (ITO) covered glass plates are separated by a distance d of approximately 75 μm by spacers in UV curable glue, and the volume between the electrodes is filled with the PMMA dispersion. The laser is focused on the mid-plane between the two electrodes, where a single PMMA particle is optically trapped. The forward scattered light is collected by the condenser (C), reflects off a 50–50 beamsplitter, and impinges on a quadrant photodiode (QPD) [Thorlabs PDQ80A]. The QPD operates at 100 kHz, providing three voltage outputs proportional to the three-dimensional displacement of the colloidal particle in the trapping volume. The z-direction corresponds to the direction orthogonal to the plane of focus. A halogen lamp (H) illuminates the sample under Köhler illumination. The white light travels through the sample in the opposite direction as the laser beam and forms an image of the particle on an Andor iXon+ EM-CCD camera. The camera is used to confirm trapping of a single particle and to align the laser inside the sample. Measurements are executed with a sinusoidal voltage difference (V) applied across the ITO electrodes either at 5 kHz frequency and 100 V amplitude or at 2 kHz frequency and 150 V amplitude.

C. Determining the charge

The QPD transmits three voltage signals to the computer which is, for sufficiently small displacements, proportional to the three-dimensional displacement of the particle in the optical trap. From this voltage signal, the charge of the colloidal particle can be calculated in three steps, elaborated

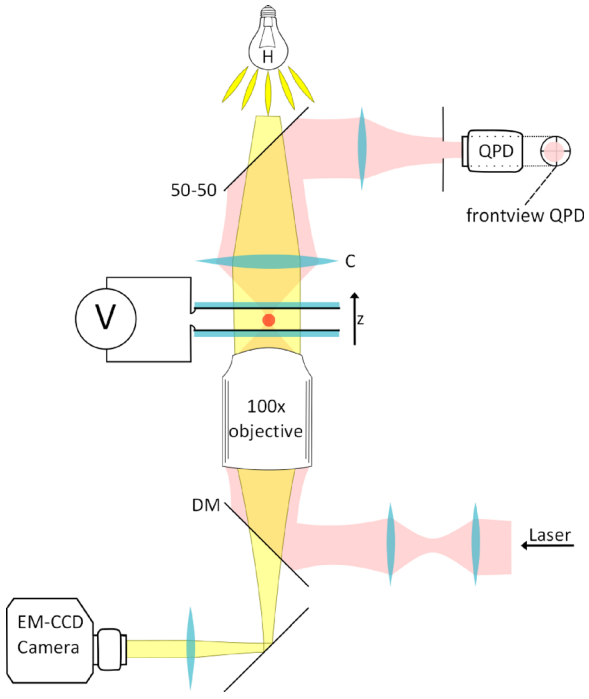

FIG. 1. Schematic overview of the OTE setup, showing the path of the IR laser beam (pink) that traps the particle and arrives at the QPD and the path of the white illumination (yellow) from the lamp to the EM-CCD camera.

below in more detail. In the first step, the voltage signal V is converted to a displacement z, by scaling the high-frequency components in the z-signal of the QPD signal to the expected high-frequency components of the Brownian displacement.[23] The latter one is obtained from the initial estimation of the particle radius r_i (provided by the supplier) and the viscosity η of the solvent. In the second step, an initial estimation of the particles charge Q_i is obtained, based on the magnitude of the frequency component of the position z at the frequency f_E of the applied sinusoidal electric field E. In the third step, a correction factor k_s is determined to adjust the mismatch between the initial estimate of the particle's radius r_i and charge Q_i and the actual (corrected) radius r_c and charge Q_c. An accurate correction is possible because we know that the corrected particle charge Q_c should be a multiple of the well-known elementary charge e. The charge Q_c is determined for each 1 s interval over a duration of several hundred seconds. In Fig. 2, we see that even after this correction, the data points do not perfectly coincide with integer values. That is because we limited the time interval to calculate the charge to 1 s. Though a longer time window to calculate Q_c would reduce this noise, the time window needs to remain much lower than the average time in between (dis)charging events or we will lose the possibility to resolve single (dis)charging events.

The data analysis procedure is illustrated in Fig. 2. First, for each particle the optical trap is calibrated according to the procedure described in Ref. 23 The average of the voltage outputs of the four photodiode quadrants is assumed to be proportional with the z-coordinate of the trapped particle. To calculate the conversion factor and to convert the voltage signal of the QPD to the displacement of the colloidal particle, we analyze Eq. (1). This equation describes the motion of the trapped particle in the z-direction, ignoring acceleration

$$QE\cos(2\pi f_E t) + F_{stoch}(t) - \kappa z - \gamma \frac{dz}{dt} = 0, \qquad (1)$$

where κ is the spring constant of the optical trap, $\gamma = 6\pi\eta r$ is the Stokes drag coefficient which is proportional to the radius r of the particle and the viscosity η of the medium, Q is the electrical charge of the particle, $E = V_{app}/d$ is the amplitude, and f_E is the frequency of the applied electric field. $F_{stoch}(t)$ is the stochastic force, with average value 0 and power spectral density $S_{FF} = 2kT\gamma$, which leads to Brownian motion. The Fourier transform of this equation, assuming that the charge Q is constant, yields $-(\kappa - i2\pi f\gamma)\,\tilde{z} + QE\delta(f - f_E) = -\tilde{F}_{stoch}$. For frequencies $f \neq f_E$, the equation simplifies to:$-(\kappa - i2\pi f\gamma)\tilde{z} = -\tilde{F}_{stoch}$. For these frequencies, the estimated value of the power spectral density is given by $S_{ZZ} = \frac{S_{FF}}{\kappa^2 + 4\pi^2\gamma^2 f^2} = \frac{kT}{2\pi^2\gamma\left(f_c^2 + f^2\right)}$, where the corner frequency is defined as $f_c = \kappa/2\pi\gamma$, which is about 10 Hz in our experiments. For frequencies much larger than the corner frequency, $f \gg f_c$, where the influence of the trap is negligible, the power spectral density multiplied by f^2 is expected to be a constant, corresponding to free Brownian motion: $S_{ZZ}f^2 = \frac{kT}{2\pi^2\gamma}$. This value can be used to convert the

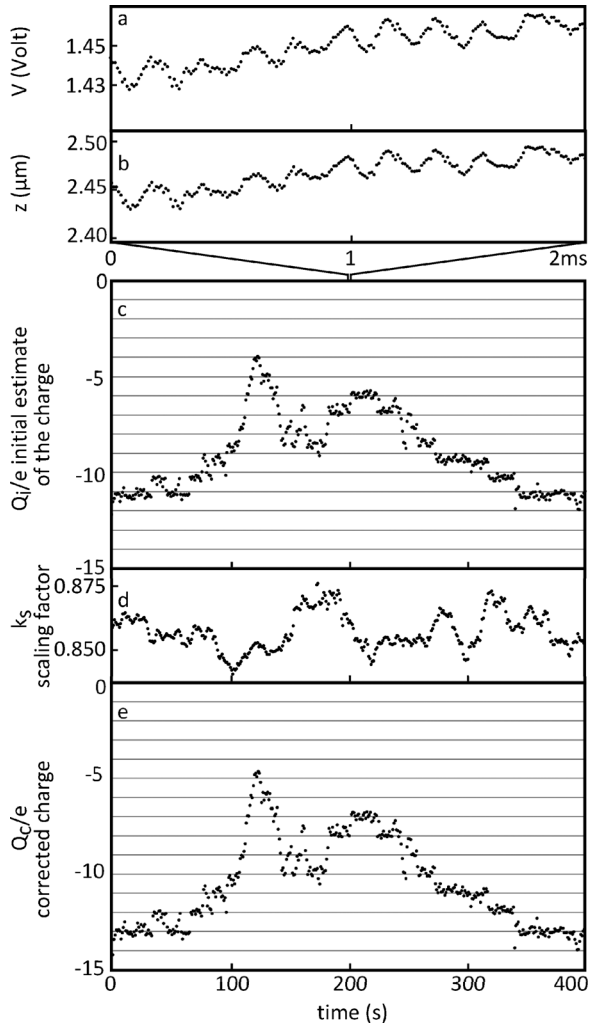

FIG. 2. Single particle measurement data and steps of the analysis. (a) z-voltage signal measured by the QPD, (b) estimated z-coordinate after scaling with the Brownian mobility, (c): normalized initial particle charge Q_i/e estimated from 100 000 z-values, (d): correction factor k_s to adjust for the actual particle size and measurement fluctuations. (e) normalized corrected particle charge obtained by dividing the initial estimate of the charge by the scaling factor, $Q_c = Q_i/k_s$; the corrected and normalized charge Q_c/e data are centered around integer values.

measured voltage V of the QPD to the z-displacement by Eq. (2), which has been derived by Flyvbjerg[24]

$$z = \sqrt{\frac{S_{ZZ}f^2}{S_{VV}f^2}}V = \sqrt{\frac{kT}{2\pi^2\gamma S_{VV}f^2}}V, \qquad (2)$$

where $S_{VV}f^2$ is the high-frequency plateau value of the power spectral density of the QPD voltage signal multiplied with the frequency squared. For each 1 s time interval, $S_{VV}f^2$ is calculated from a time window of minimum 21 s, centered around the considered 1 s time interval. The time window is optimized for each measurement and needs to be larger than the mean time between charging events. To determine γ, the initial estimate $r_\mathrm{i} = 0.5\,\mu$m provided by the manufacturer is used.

The force equation in Eq. (1) implicitly used the Hückel approximation,[25] which is valid on the condition that $\kappa_D r \ll 1$, where κ_D^{-1} is the Debye length and r is the radius

of the particle. This approximation holds for all experiments presented in this paper. From transient current measurements,[26] we determined the concentration of charged inverse micelles in the solvent. Below the CMC, the concentration of charged inverse micelles is below our detection limit. For these concentrations, we obtain an upper limit for the concentration of charged inverse micelles of $\overline{n} = 3.0 \times 10^{17}\,\mathrm{m}^{-3}$. This corresponds to $\kappa_D r = 0.16$, which satisfies the condition for the Hückel approximation. The solution with highest concentration of surfactant in this study contains 0.05 wt. % OLOA 11000 in dodecane. In this solution, the concentration of charged inverse micelles is $\overline{n} = 3.3 \times 10^{18}\,\mathrm{m}^{-3}$ and $\kappa_D r = 0.55$. Therefore, in order to be able to use the Hückel approximation, the measurements with surfactant concentration above the CMC are carried out with a small DC offset of 1 V in order to deplete charged inverse micelles from the bulk and to reduce $\mathrm{kR} = 3.10^{-4} \ll 1$.

An initial estimate of the particle charge Q_i is made according to Eq. (3), which is derived from Eq. (1), for each time interval of $\Delta t = 1$ s (Ref. 20)

$$Q_i = \frac{2\pi\gamma f_{s,Q}}{E}\left(2\pi f_c Re(\hat{z}_E) + 2\pi f_E Im(\hat{z}_E)\right), \tag{3}$$

where $f_{s,Q} = 1$ Hz is the frequency at which the charge is calculated and $\hat{z}_E$ is the Fourier component of the particle z–position for the frequency $f = f_E$.

If the measurement is executed with accuracy higher than the elementary charge e, and the charge on the particle does not change within a time interval, then the Q_i value should be a multiple of the unit charge e. However, because the initial parameters, such as the radius r, are not exactly known, the obtained Q_i values are typically not multiples of e, but rather multiples of $e' = k_s e$, with k_s a correction factor that can be determined from the measurements. In order to find the best value for k_s, we calculated the residue over an interval of minimum 21 s as a function of k[19]

$$R^2(k, t_0) = \sum_{t=t_0-n.\Delta t}^{t_0+n.\Delta t}\left(\frac{Q_i(t)}{e} - \left[\frac{Q_i(t)}{ke}\right]ke\right)^2, \tag{4}$$

where Δt is 1 s and n is minimum 10. $Q_i(t)$ is the charge at time t and $[Qi(t)/ke]$ denotes rounding to the nearest integer. k_s is the optimal value of k where the residue $R^2(k, t_0)$ reaches a local minimum. The value of k_s depends on the data point it is calculated for and on the size of the time interval $2n\Delta t$, with $\Delta t = 1$ s, around it that is taken into account. The larger the value for n, the lesser it makes up for fluctuations in the sensitivity of the measurement. When n is too large, part of the data is not clustered around integer values, which leads to incorrectly identifying charging and discharging events. The size of n also determines the amount of data that has to be discarded. After all, for the first and last n data points of each measurement, k_s cannot be calculated. Hence, this part of the data cannot be used. When calculating the residue of a charge measurement, the parameter n is chosen such that $n.\Delta t$ is larger than the mean time in between charging events of that measurement.

Figure 3 shows an example where $R^2(k)$ is calculated for a set of Q_i values over a 201 s time interval centered around a particular value of t_0. The presence of a prominent local minimum significantly below the trend k^2e^2 at the value $k = k_s$ acts as an objective test to check whether the charge is measured with precision higher than the elementary charge. The fact that this value is different from unity indicates that some of our assumptions concerning the particle size, the distance between the electrodes, or other assumptions are not correct. As shown in Fig. 2(d), the correction factor k_s fluctuates slightly over time, suggesting that some measurement parameters fluctuate over time. A condition has to be imposed to prevent that the introduction of a correction factor that varies over time could introduce discrete jumps in the charge measurement that could be interpreted as a charging or discharging event. Therefore, the variation between consecutive correction factors should remain small enough, so that the product of the difference between consecutive correction factors and the value of the particle's charge is smaller, half the elementary charge $\left|k_s(t) - k_s(t+1)\right|Q_i(t) < \frac{1}{2}e$.

Finally, we can estimate the corrected particle charge $Q_c = Q_i/k_s$, for which all data points are scattered around multiples of e. The normalized, corrected charge Q_c/e is shown in Fig. 2(e).

III. RESULTS AND DISCUSSION

In previous work, the charging and discharging of particles in pure dodecane (without surfactant) has been studied.[20] Here, the influence of added surfactant on the dynamic charging of PMMA particles is investigated with precision higher than the elementary charge.

In this section, the charging of single PMMA particles in dodecane is studied for different concentrations of the commercial surfactant OLOA 11000. The studied concentrations span from 0.001 wt. % to 0.05 wt. %, which includes the CMC around 0.005 wt. %.[22] The charging behavior above and below this concentration is observed to be distinctly different. Also, the particle charge measurements are carried out in the absence or in the presence of a small DC offset to the applied voltage ($V_{DC} = 1$ V). The application of a small DC voltage offset expands the range of concentrations at which the charge of a particle can be measured with elementary charge resolution.

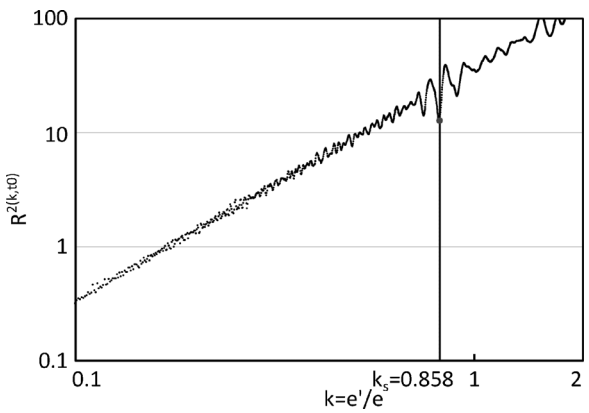

FIG. 3. The residue $R^2(k, t_0)$ plotted for the example. The local minimum indicates that the measured charges Q_i are multiples of $k_s e$, in this case of 0.858 e.

The experimental results are divided into four separate subsections. First, charge measurements in solutions close to the CMC with DC offset are discussed. These measurements show a particle charge that fluctuates around a mean charge value. Second, we present the charge measurement of a particle in a solution below the CMC, first with and then without DC voltage. Here, the particle's charge is not stable and positive charge accumulates on the particle over time. In Sec. III C, the influence of the DC offset is discussed. In Sec. III D trends in the charging behavior of the colloidal particles with 1 V DC offset as a function of the surfactant concentration are analyzed.

Some of the observations that are presented in this paper are not in line with earlier publications, in particular, the publications by Strubbe *et al.*[19] and Beunis *et al.*[20] Therefore, before we can delve into the experimental results, we have to address some key differences between these experiments and the earlier ones. There are two important distinctions to make with respect to experimental work from Strubbe (Ref. 19). First, the particles that were investigated here were freely diffusing; hence, the experiment was much shorter, making it harder to detect whether the particles undergo the same effects as they do in this work. Second, the particles from Ref. 19 are silica particles. The different chemical composition may cause particles to behave differently. The differences with the work of Beunis (Ref. 20) lie mainly in the fabrication method of the microfluidic cell. Here, the cell consists of two ITO-covered glass plates that have been cleaned in a cleanroom with deionized (DI)-water, RBS, acetone, isopropanol, and again with DI-water, whereas the double folded aluminum foil strips that serve as electrodes in Ref. 20 cannot be cleaned this way. Because we attempt to work in pure dodecane, this is a likely source of contamination. Indeed, the results from Ref. 20 mirror the results that we present for high concentrations of surfactant, solidifying this assumption.

A. Particle charge fluctuations close to the CMC with DC offset

Figure 4 displays the variation of the charge of a single particle over time in a mixture of 0.0046 wt. % OLOA in dodecane which is near the CMC. The applied voltage across the electrodes, separated by 75 μm, has an AC amplitude of 100 V, a frequency of 5 kHz, and a DC offset of 1 V. The charge histogram reveals the discrete nature of the charge and that there is an approximately normal distribution around an average value of -12.

To determine the number of charging events, the normalized charge Q_c/e is rounded to the nearest integer value. When two consecutive integer values are not equal, this represents a charging event. The time sequence of Fig. 4 contains 499 charging (or discharging) events which are defined with an accuracy of 1 s, the time interval for each charge measurement. Charging events much faster than 1 s can be ruled out if a local minimum corresponding to the elementary charge is detected in $R^2(k,t)$.

The average time in between consecutive charging events in Fig. 4 is 5.01 s. Figure 5 displays the histogram of

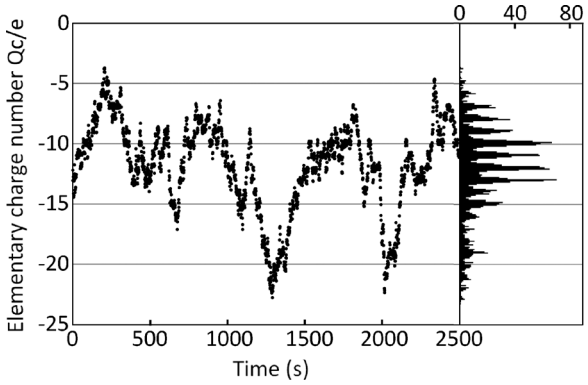

FIG. 4. (left) Time evolution of the normalized charge Q_c/e for a single PMMA particle in dodecane with 0.0046 wt. % OLOA 11 000 during 2500 s (one charge measurement per second). The charge fluctuates around the average value of -12. (right) Charge histogram from 2500 values, 10 intervals per unit charge, showing the discrete nature of the particle charge.

the time between consecutive charging events for the time sequence in Fig. 4. The linear slope in the semi-logarithmic plot (inset) reveals that the charging and discharging events follow a Poisson distribution (similar as observed in Ref. 20). This signifies that consecutive charging events are uncorrelated.

B. Particle charging below the CMC with DC offset

For surfactant concentrations below 0.003 wt. %, the charging mechanism is different than around the CMC (0.005 wt. %) shown in Sec. III A. A representative measurement at 0.0015 wt. % is shown in Fig. 6. It is evident that the charge does not fluctuate around a mean value. Instead, the charge steadily increases over time (in Fig. 6 there is only one exception around 400 s). It is also apparent that the charging frequency is lower: there are only 28 events over 1600 s, yielding an average time in between consecutive charging events of 57 s.

A similar behavior is observed for all measurements with OLOA concentrations well below the CMC. The charge becomes more positive, and the mean time between events is larger than 10 s.

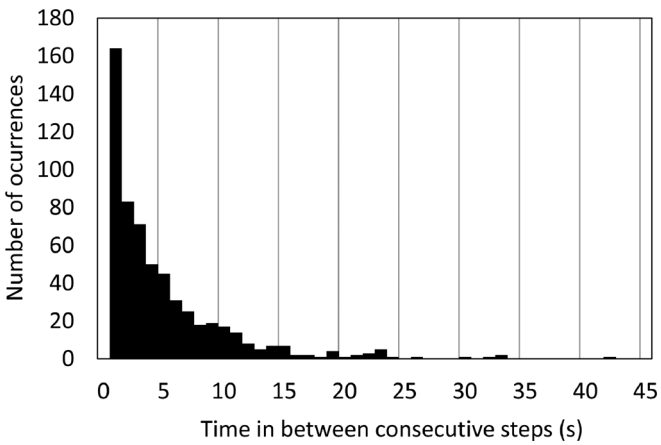

FIG. 5. Histogram of the 499 time intervals in between consecutive charging events of a 1 μm PMMA particle in dodecane with 0.0046 wt. % OLOA 11 000 during 2500 s (corresponding to Fig. 4). The average value is 5.01 s. Inset: the histogram shown in a semi-logarithmic diagram.

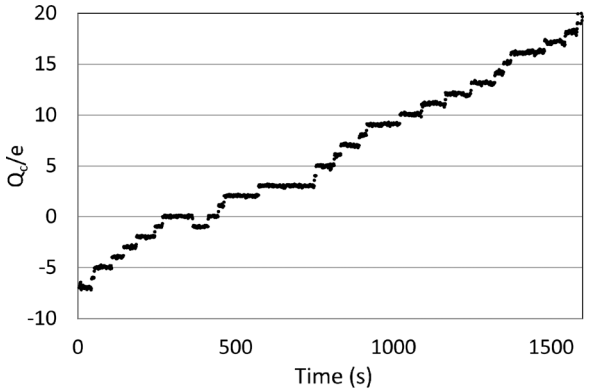

FIG. 6. Time evolution of the charge of a $r = 0.5\,\mu$m PMMA particle dispersed in dodecane with 0.0015 wt. % of OLOA 11 000 with $V = 100\,V$ at *5 kHz* and 1 V DC offset. The particle charge increases at about 1 elementary charge per 57 s.

C. Particle charging without DC offset

The variation of the charge of PMMA particles in surfactant concentrations has been investigated without an electric DC offset. For concentrations below 0.003 wt. % OLOA 11 000 in dodecane, the presence of a DC offset has no significant influence on the charging dynamics. In Fig. 7, the particle charge is shown in function of time over a 600 s interval for a mixture with 0.0015 wt. % OLOA 11000 in dodecane. The particle charge increases monotonously and the mean time between events is more than 10 s.

When the surfactant concentration is increased to 0.003 wt. %, the DC component has an important effect on the charging behavior. To illustrate this, the charge of the same particle is measured over 600 s for different DC values in Fig. 8, starting with 0 V and increasing stepwise by 0.25 V. In between the measurements, the particle is kept trapped while short-circuiting the electrodes during 600 s in order to let it return approximately to the same initial charge value.

Two different charging behaviors can be observed. When the applied DC voltage is below 0.5 V, the charge Q_C fluctuates around a mean (negative) charge. A similar behavior was observed for measurements where a DC voltage was applied, at slightly higher surfactant concentrations as shown in Fig. 4. When the DC voltage is increased to 0.5 V or

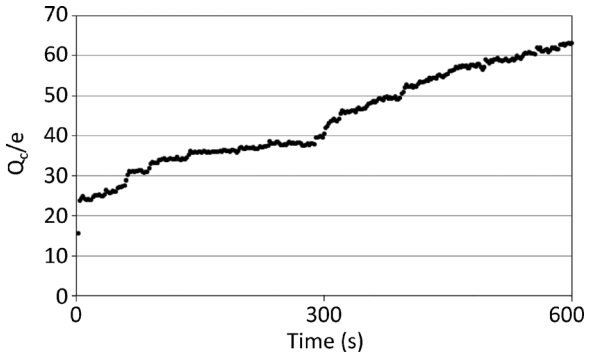

FIG. 7. Time evolution of the charge of a r = 0.5 μm PMMA particle dispersed in dodecane with 0.0015 wt. % of OLOA 11 000 with $V = 100$ V at 5 kHz and 0 V DC offset.

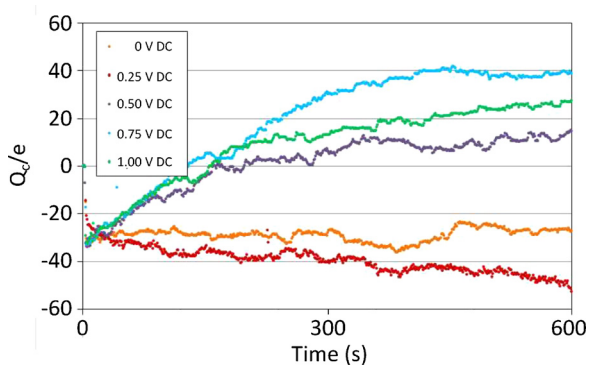

FIG. 8. The charge of a $r = 0.5\,\mu$m PMMA particle in dodecane with 0.003 wt. % OLOA 11 000 with $V = 100$ V at 5 kHz. The particle charge is measured for 5 different values of the DC voltage offset from 0 V DC up to 1 V DC. All measurements are performed on the same particle. The elementary charge resolution is not obtained for measurements with $V_{DC} < 0.5$ V. For these measurements, the mean value of the conversion factor k_s from the other measurements with $V_{DC} \geq 0.5$ V is used in this graph. [For the first data point, some measurements show anomalous behavior. This is because the voltage amplifier is switched on manually after several seconds.]

higher, the charge increases over time. Another important distinction between $V_{DC} < 0.5$ V and $V_{DC} \geq 0.5$ V is that for small DC voltages the particle charge can no longer be observed with elementary charge resolution because the charge data are noisier.

D. Influence of surfactant concentration on the charging behavior with DC offset

Despite the difference in charging behavior below and above the CMC, some trends are visible over the entire concentration range. Figure 9 shows charge measurements for 12 different surfactant concentrations, with the size of each dot being proportional to the fraction of time that the particle carried the indicated charge. For all measurements, a DC offset of 1 V is applied. Below the CMC (red vertical line), the final charge (red dot) is typically higher than the initial charge (blue dot), which corresponds to measurements where the charge increases monotonously. Above the CMC, the charge fluctuates around an average value. It is therefore speculated that the presence of inverse micelles can stabilize the charging and discharging processes.

For surfactant concentrations above the CMC, the time evolution is entirely different. The probability distribution is Gaussian-like. Charges are mostly negative and there does not seem to be a correlation between the mean charge and the concentration of surfactant.

Inverse micelles are known to play an important role in charge stabilization.[3,4] It is also well known that the addition of surfactant increases the concentration of charged and uncharged inverse micelles in nonpolar solvents.[27,28] Therefore, if the particle charging is related to interactions with charged or uncharged inverse micelles, one can expect that the increase of surfactant concentration should be accompanied with a decrease in the average time in between consecutive charging events. This is indeed observed in Fig. 10. The average time interval between successive charging events drops by an order of magnitude when the concentration is increased from the lowest to the highest

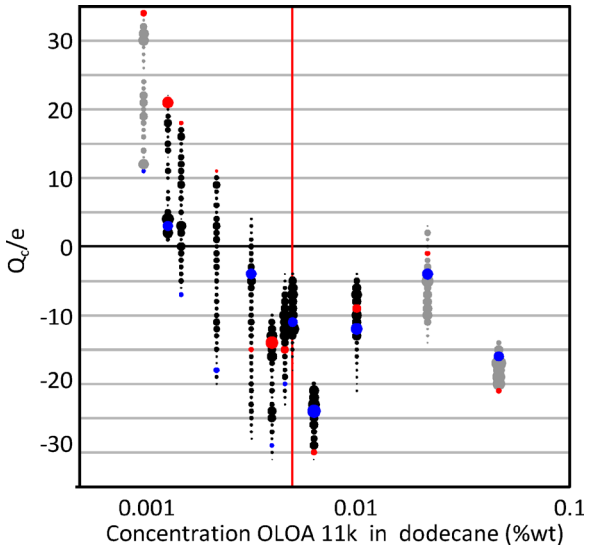

FIG. 9. Variation of the particle charge with time for different concentrations of the surfactant OLOA 11k, all measured with 1 V DC offset. The blue and red dots correspond to the initial and final values of the particle charge. The area of each dot is proportional to the fraction of the time that the particle carried the indicated charge. The red vertical line at 0.005 wt. % indicates the CMC. For the measurements with black dots, the AC voltage has a 100 V amplitude at 5 kHz and for measurement with grey dots the AC voltage is 150 V at 2 kHz.

concentration. The charge is calculated once every second, implying that charging time intervals shorter than 1 s (which may be present at higher concentrations) cannot be detected.

E. Discussion

The charging of PMMA particles behaves differently below and above the CMC, and the presence of a DC voltage has an influence on the charging behavior. First we discuss the charging behavior of particles below the CMC.

The charging behavior of PMMA particles in dodecane with surfactant concentrations lower than 0.003 wt. %, below the CMC of 0.005 wt. %, exhibits a clear trend (see Figs. 6 and 7). During application of an AC field, the charge on the particle becomes more positive. When a DC voltage of 1 V is applied across the electrodes, the bulk is completely depleted of ionic particles such as charged premicellar

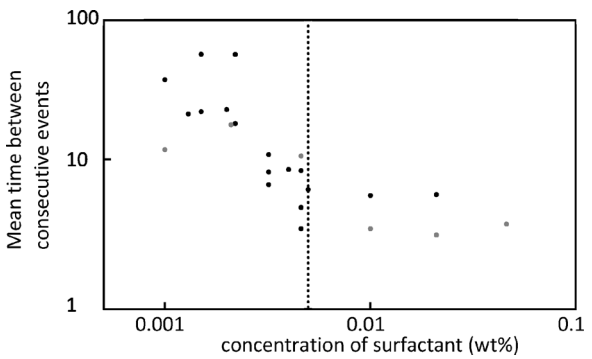

FIG. 10. Mean time between consecutive charging events as a function of the weight fraction of surfactant, measured while applying a 1 V DC offset. The vertical line at 0.005 wt. % indicates the value of the CMC. For black dots, the applied voltage is 100 V at 5 kHz and for grey dots the voltage is 150 V at 2 kHz.

aggregates, just as that observed in the case of charged inverse micelles.[26] Under these conditions, a similar increase of the particle charge is observed. This observation of a similar charging with or without DC voltage disfavors a charging mechanism in which a PMMA particle adsorbs positively charged ions preferentially from its environment since in the presence of a DC voltage the concentration of positive charges near the particle is considerably lower than without DC voltage. Instead, supported by measurements without surfactant showing similar charging behavior (not shown), it rather suggests that a PMMA particle sheds negative charges over time [see Fig. 11(a)] due to the extremely large electrical fields in the order of MVm^{-1}. Such a field-induced, non-equilibrium charging process does not involve surfactant molecules.

The increase of surfactant concentration from 0.001 wt. % to 0.003 wt. % results in a decrease in the mean time between elementary (dis)charging events for particles that are monitored under 100 V AC field with a 1 V offset. The higher frequency of charging and discharging events for higher concentrations reveals that there is a second mechanism that involves single surfactant molecules, shown in Fig. 11(b). Here, positively (top) or negatively (bottom) charged species stabilized by surfactant molecules are removed from the particle in the presence of a field. The inverse process in which stabilized charges are adsorbed onto the particle surface is ignored here because the bulk concentration of such free charges is extremely low. Therefore, the proposed charging below the CMC is a combination of field-induced stripping of negative charge and surfactant-mediated removal of charge. The surfactant concentration also has an effect on the initial charge of the colloidal particle (see Fig. 9). For very low surfactant concentrations, the initial charge is positive ($\sim$10e). For concentrations above 0.002 wt. % OLOA 11000 in dodecane, the initial charge is negative (~ -10e).

The application of a DC offset decreases the noise in the charge data. In the measurements shown in Fig. 8, the standard deviation of the normalized charge data around integer values increases when the DC voltage decreases from $\sigma_{1\,V} = 0.16\ e$ for 1 V to $\sigma_{0.5\,V} = 0.43\ e$ for 0.5 V. Because both measurements are performed on the same particle with identical laser alignment, the increase in the standard deviation can be attributed to the decrease in DC voltage. We assume that the noise in the motion of the PMMA particle is related to the (variable) interaction with a small number of charged molecules or charged premicellar aggregates below the CMC and charged inverse micelles above the CMC. This interaction leads to the well-known retardation effect when a large number of charges are present. It has been shown that by applying a DC offset voltage, charges can be stripped off the double layer around a particle, leading to a reduction in the retardation force.[29] In the limit of low particle charges, the interaction between a particle and a low number of countercharges can lead to fluctuations in its motion. By applying a DC offset, a small number of charges are present near the PMMA particle; hence, the noise reduces. The range of surfactant concentrations where the particle's charge can be measured with unitary resolution is then extended from

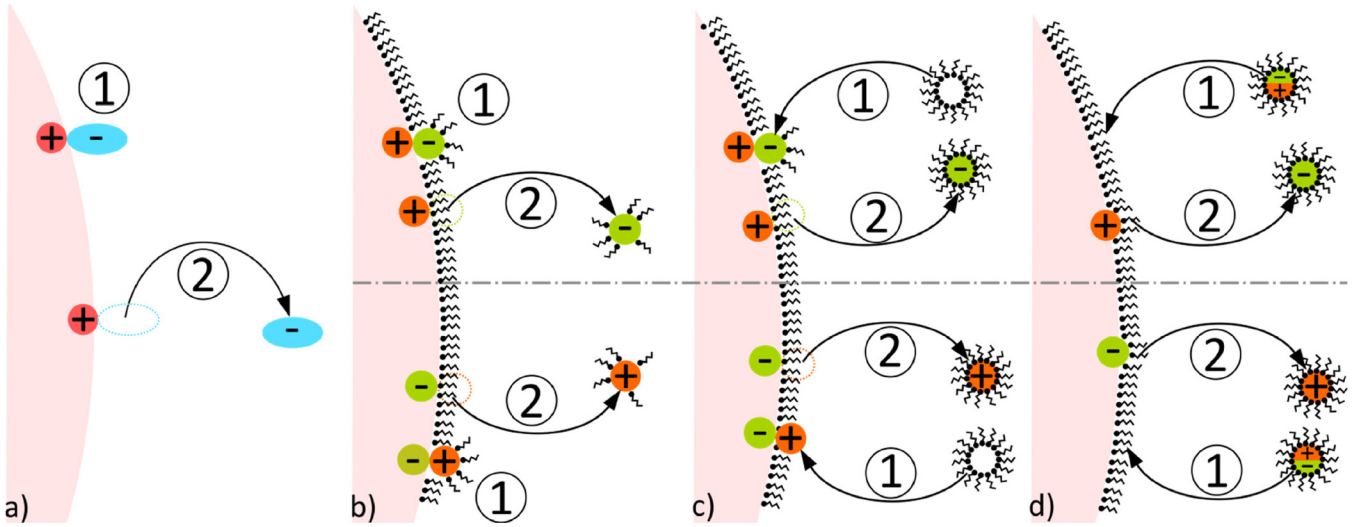

FIG. 11. Charging mechanisms. (a) In a field induced charging mechanism, negatively charged surface groups are stripped from the particle. (b) Surfactant molecules facilitate surface charging and discharging and form premicellar aggregates with ionic molecules. (c) and (d) Neutral inverse micelles charge or discharge the particle by either supplying or removing ionic molecules.

about 0.004 wt. % to 0.05 wt. %, which is one order of magnitude above the CMC.

Charge measurements of particles in solvents with surfactant concentrations larger than 0.003 wt. % do not show an increase in charge. Instead, the particle charge fluctuates around a mean charge value and the charging/discharging events are more frequent than at lower concentrations. At these surfactant concentrations, inverse micelles are present in the bulk liquid. Due to the DC offset, the bulk is depleted off charged inverse micelles, ignoring a low concentration of newly generated charges.[30] This introduces two additional mechanisms through which surfactant can contribute to particle charging and discharging by supplying as well as removing ionic species from the particle surface, as shown in Figs. 11(c) and 11(d). Here, charge-regulation could play an important role. In thermodynamic equilibrium, the particle charge will then fluctuate around an equilibrium value. If the particle charge deviates from the average value, electrostatic interaction will favor those processes of charging leading towards the average value. Therefore, even if the mechanisms from Figs. 11(a) and 11(b) are still occurring, the dominant effect would likely be the charge stabilization due to inverse micelles of Figs. 11(c) and 11(d). From the exponential shape of the histogram of times in between consecutive charging events, we know that the charging/discharging is a Poisson process, indicating that successive charging events are uncorrelated.

In summary, three mechanisms have been proposed to explain charging below and above the CMC: the field-induced stripping of negative charges from the PMMA particle when an AC voltage is applied, surfactant-mediated charge desorption, and charging mediated by inverse micelles.

IV. CONCLUSION

Understanding the charging behavior of colloidal particles in surfactant rich environments is of interest for a varied field of industrial applications based on colloidal systems.[1–4] Though the charging mechanisms of several specific surfactant enriched colloidal systems have been identified,[6,14–18] a general, predictive framework for colloidal systems is still lacking. This is partially because existing measurement tools can provide only limited information on the charging behavior. In this paper, we demonstrate the use of optical trapping electrophoresis to detect elementary charging events on single colloidal PMMA particles for the nonpolar liquid dodecane containing surfactant (OLOA 11000).

We show that the technique is effective for surfactant concentrations both below and above the critical micelle concentration, and with or without DC offset voltage. The analysis of discrete charging events in equilibrium or out of equilibrium provides insight into the charging mechanism at different surfactant concentrations.

Without a DC voltage, the particle charge is measured with elementary charge resolution for surfactant concentrations up to 0.003 wt. %. By adding a 1 V DC offset, this range is extended to 0.05 wt. %, which is above the CMC at 0.005 wt. %. This can be understood from the interaction between particles and countercharges which move in opposite directions in an electric field, which dampens the oscillation of the particle. This effect is known as the retardation effect.

Below the CMC, particles gradually lose negative charges during the mobility measurement. For particles in solutions at concentrations around the CMC or higher, we observe that the particle's charge becomes stable and fluctuates around a mean charge value. This indicates that at these concentrations the charging related to inverse micelles dominates the charging behavior of the colloidal particles. As the concentration of surfactant increases, the mean time between consecutive charging events decreases both above and below the CMC. This suggests that both individual surfactant molecules and inverse micelles can be involved in charging mechanisms in nonpolar liquids.

ACKNOWLEDGMENTS

This work is financially supported by the Research Foundation Flanders (FWO).

[1]B. Comiskey *et al*., Nature **394**, 253 (1998).
[2]H. J. Spinelli, Adv. Mater **10**, 1215 (1998).
[3]P. H. C. Vanderhoeven and J. Lyklema, Adv. Colloid Interface **42**, 205 (1992).
[4]W. Ryoo *et al*., Langmuir **21**, 5914 (2005).
[5]F. Strubbe, F. Beunis, and K. Neyts, J. Colloid Interface Sci. **301**, 302 (2006).
[6]G. S. Roberts *et al*., Langmuir **24**, 6530 (2008).
[7]M. Karvar *et al*., Langmuir **30**, 12138 (2014).
[8]M. M. Gacek and J. C. Berg, J. Colloid Interface Sci. **449**, 192 (2015).
[9]J. Schmidt *et al*., J. Colloid Interface Sci. **3**, 86 (2012).
[10]M. Karvar *et al*., Langmuir **27**, 10386 (2011).
[11]B. J. Bleier *et al*., J. Colloid Interface Sci. **4**, 93 (2017).
[12]B. A. Yezer *et al*., J. Colloid Interface Sci. **4**, 49 (2015).
[13]M. M. Gacek and J. C. Berg, Electrophoresis **35**, 1766 (2014).
[14]I. D. Morrison, Colloid Surf. A **71**, 1 (1993).
[15]M. F. Hsu, E. R. Dufresne, and D. A. Weitz, Langmuir **21**, 4881 (2005).
[16]R. Kemp *et al*., Langmuir **26**, 6967 (2010).
[17]S. Poovarodom and J. C. Berg, J. Colloid Interface Sci. **346**, 370 (2010).
[18]G. N. Smith, J. E. Hallett, and J. Eastoe, Soft Matter **11**, 8029 (2015).
[19]F. Strubbe, F. Beunis, and K. Neyts, Phys. Rev. Lett. **100**, 218301 (2008).
[20]F. Beunis *et al*., Phys. Rev. Lett. **1**, 08 (2012).
[21]L. Antl *et al*., Colloid Surf. **17**, 67 (1986).
[22]F. Beunis *et al*., Appl. Phys. Lett. **97**, 181912 (2010).
[23]R. Galneder *et al*., Biophys. J. **80**, 2298 (2001).
[24]I. M. Tolic-Norrelykke, K. Berg-Sorensen, and H. Flyvbjerg, Comput. Phys. Commun. **1**, 59 (2004).
[25]A. V. Delgado *et al*., J. Colloid Interface Sci. **3**, 09 (2007).
[26]A. R. M. Verschueren *et al*., J. Phys. Chem. B **1**, 12 (2008).
[27]Q. Guo, V. Singh, and S. H. Behrens, Langmuir **26**, 3203 (2010).
[28]A. S. Dukhin and P. J. Goetz, J. Electroanal. Chem. **588**, 44 (2006).
[29]F. Strubbe *et al*., Phys. Rev. X **3**, 021001 (2013).
[30]F. Strubbe, M. Prasad, and F. Beunis, J. Phys. Chem. B **119**, 1957 (2015).